Inorganic Chemistry
Forum Article

Inorg. Chem. **2010**, *49*, 3567–3572 **3567**
DOI: 10.1021/ic900798q

Enzymatic versus Inorganic Oxygen Reduction Catalysts: Comparison of the Energy Levels in a Free-Energy Scheme

Christian H. Kjaergaard, Jan Rossmeisl,* and Jens K. Nørskov

Center for Atomic-scale Materials Design (CAMD), Department of Physics, Nano DTU Technical University of Denmark, Lyngby 2800, Denmark

Received April 24, 2009

In this paper, we present a method to directly compare the energy levels of intermediates in enzymatic and inorganic oxygen reduction catalysts. We initially describe how the energy levels of a Pt(111) catalyst, operating at pH = 0, are obtained. By a simple procedure, we then convert the energy levels of cytochrome *c* oxidase (CcO) models obtained at physiological pH = 7 to the energy levels at pH = 0, which allows for comparison. Furthermore, we illustrate how different bias voltages will affect the free-energy landscapes of the catalysts. This allows us to determine the so-called theoretical overpotential of each system, which is shown to be significantly lower for the enzymatic catalysts compared to the inorganic Pt(111) catalyst. Finally, we construct theoretical polarization curves for the CcO models, in order to illustrate the effect of the low overpotentials on turnover rates per site.

Introduction

Fuel cells are receiving considerable interest as efficient devices for the transformation of chemical energy into electrical energy. In the proton-exchange membrane (PEM), hydrogen/oxygen fuel cell hydrogen is oxidized at the anode, releasing protons and electrons, which are then recombined at the cathode, where gaseous dioxygen is converted into water.[1] Despite its promising features, the full potential of this system is still to be realized, mainly because of the fact that the cathode reaction is slow. This means that the fuel cell must be run at a potential considerably less than the ideal for hydrogen oxidation even for the most efficient precious metal catalyst, Pt.[1,2] This issue is overcome in nature, where enzymatic oxygen reduction is known to occur at very low overpotentials.[3] Two groups of enzymes are particularly important with regard to oxygen reduction: the cytochrome *c* oxidases (CcOs) and the multicopper oxidases (MCOs). In fact, MCOs have already been employed in enzymatic fuel cells, where experiments have revealed overpotentials in laccase as low as 0.1 V for oxygen reduction.[4]

It would be highly desirable if we could design a cathode material with electrocatalytic properties similar to those of the enzymes. In that way, one could combine the low overpotential of the active sites of the enzymes with the high surface density of the active sites of the inorganic cathode materials. However, in order to be inspired by the functionality of the enzymes, one must be able to compare the catalytic features of the inorganic catalyst with those of the enzyme. The challenge is that the working conditions and reaction mechanisms of the biological and inorganic catalysts are quite different. In the present paper, we introduce a method based on published density functional theory (DFT) calculations that allows for a direct comparison of the free-energy levels of intermediates in the reaction over the two types of catalysts. It opens the possibility of ranking the catalytic activities at normal PEM fuel cell operating conditions.

Free-Energy Method for Comparing Catalysts

Pt(111) and Pt Alloys. The approach we take is very simple and has been introduced to understand the trends in catalytic activities as a function of the potential and catalyst for transition-metal surfaces.[5−7] The oxygen reduction reaction (ORR) over a Pt(111) surface consists of a sequence of additions of electrons and protons to dioxygen:

$$O_2(g) + * + (H^+ + e^-) \rightarrow OOH* \quad (1)$$

$$OOH* + (H^+ + e^-) \rightarrow H_2O(l) + O* \quad (2)$$

*To whom correspondence should be addressed. Email: jross@fysik.dtu.dk.

(1) Markovic, N. M.; Ross, P. N. *CATTECH* **2000**, *4*, 110–126.
(2) Hoogers, G.; Thompsett, D. *CATTECH* **1999**, *3*, 106–124.
(3) Ferguson-Miller, S.; Babcock, G. T. *Chem. Rev.* **1996**, *96*, 2889–2907.
(4) Mano, N.; Soukharev, V.; Heller, A. *J. Phys. Chem. B* **2006**, *110*, 11180–11187.
(5) Nørskov, J. K.; Rossmeisl, J.; Logadottir, A.; Lindqvist, L.; Kitchin, J.; Bligaard, T.; Jónsson, H. *J. Phys. Chem. B* **2004**, *108*, 17886–17892.
(6) Rossmeisl, J.; Logadottir, A.; Nørskov, J. K. *Chem. Phys.* **2005**, *319*, 178–184.
(7) Rossmeisl, J.; Dimitrevski, K. P.; Siegbahn, P. E. M.; Nørskov, J. K. *J. Phys. Chem. C* **2007**, *111*, 18821–18823.

Published on Web 04/12/2010

$$O* + (H^+ + e^-) \rightarrow HO* \quad (3)$$

$$HO* + (H^+ + e^-) \rightarrow H_2O(l) + * \quad (4)$$

Here, * resembles a site on the Pt surface where a molecule can bond. By definition, the free energy of $(H^+ + e^-)$ at a given potential U and pH (at $T = 298$ K) is given by

$$\Delta G(U, \mathrm{pH}) = eU + k_B T \ln(10)\mathrm{pH}$$

if U is measured relative to the standard hydrogen electrode (SHE). e is the electronic charge, and k_B is the Boltzmann constant. This means that if we can calculate the free energy of adsorbed OOH, OH, and O at the water−Pt(111) interface (including local field effects outside the surface [8]), we can obtain the free energy of all intermediates in the ORR. This is illustrated in Figure 1a at pH = 0 corresponding to the acidic conditions of a PEM fuel cell. The free energy levels are shown for bias voltages of 0 and 1.23 V and the highest voltage where all reaction steps are downhill in free energy. Irrespective of any additional reaction barriers for proton transfers, this defines the potential where the thermodynamics of the intermediates start to slow down the reaction. We define the difference between the equilibrium potential (1.23 V at pH = 0) and this potential [0.78 V for Pt(111)] as the theoretical overpotential. The figure shows the origin of the large overpotential for the ORR over Pt(111). The O and OH bonds to the surface are so strong that at the equilibrium potential a large free energy is required to remove them. A surface that binds oxygen weaker, such as Au(111), will not have this problem, but now the oxygen−surface bond is so weak that the formation of OOH becomes uphill at potentials above 0.18 V. In a previous study, it was predicted that linear relationships exist between the binding energy of the various intermediates in the reaction sequence.[9] With the above-mentioned assumption of no additional barriers, it becomes possible to correlate the activity of each reaction step to a single descriptor, namely, the binding energy of atomic oxygen. This gives rise to a so-called volcano plot, as seen in Figure 1b. Here, the measured activity is plotted against the binding energy of atomic oxygen, in the same diagram as the theoretical volcano. It is seen that, on pure platinum, oxygen is bound too strongly to the surface. A large amount of research is presently devoted to finding metal alloys that bind oxygen a little weaker than Pt, and the best known inorganic electrocatalyst at the moment is a $Pt_3Ni(111)$ surface,[10,11] which binds oxygen by ~0.25 eV less than Pt(111). However, even a material at the very top of the volcano will need a substantial overpotential, which is seen for Pt, where the OOH formation is also uphill at high potential even though Pt is on the strong binding side of the volcano.

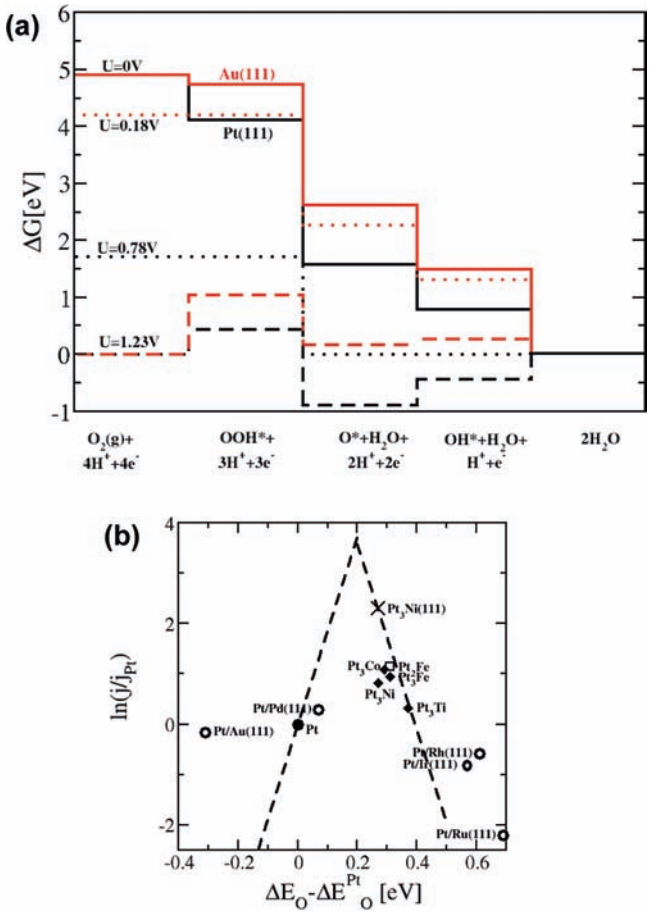

Figure 1. (a) Free-energy diagram for oxygen reduction on Pt (black) and Au (red) at $U = 0$ V (full line) and 1.23 V (dashed line) and at the potential where the least exothermic $(H^+ + e^-)$ charge-transfer step reaches equilibrium, corresponding to the theoretical overpotentials (dotted line). (b) Measured current densities for Pt-containing catalysts reported in the literature versus oxygen binding energies calculated with DFT; both axes are normalized to Pt. The data points marked with ◆ are from ref 12, the × point is from ref 10, the ○ points are from ref 13, and the □ point is from ref 14. The binding energy is in this case estimated by the binding on Pt_3Fe. The dashed lines correspond to the theoretically determined volcano plot as depicted in ref 5.

Enzymes. Of the two groups of oxygen reduction enzymes mentioned in the Introduction, we will concentrate in the following on the CcOs because here two sets of very detailed DFT calculations have been performed.[15,16] Kaukonen[15] and Blomberg and Siegbahn[16] have calculated free energies for all the intermediates in the reaction based on a bovine CcO crystal structure and various experimental data.Very recently Blomberg and Siegbahn have investigated the O to E transition;[17,18] however,

(8) Rossmeisl, J.; Nørskov, J. K.; Taylor, C. D.; Janik, M. J.; Neurock, M. *J. Phys. Chem. B* **2006**, *110*, 21833–21839.
(9) Abild-Pedersen, F.; Greeley, J.; Studt, F.; Rossmeisl, J.; Munter, T. R.; Moses, P. G.; Skulason, E.; Bligaard, T.; Nørskov, J. K. *Phy. Rev. Lett*. **2007**, *99*, 016105.
(10) Stamenkovic, V. R.; Fowler, B.; Mun, B. S.; Wang, G. F.; Ross, P. N.; Lucas, C. A.; Markovic, N. M. *Science* **2007**, *315*, 493–497.
(11) Rossmeisl, J.; Karlberg, G. S.; Jaramillo, T.; Nørskov, J. K. *Faraday Discuss*. **2008**, *140*, 337–346.
(12) Stamenkovic, V. R.; Moon, B. S.; Mayrhofer, K. J. J.; Ross, P. N.; Markovic, N. M.; Rossmeisl, J.; Greeley, J.; Nørskov, J. K. *Angew. Chem., Int. Ed.* **2006**, *45*, 2897–2901.
(13) Zhang, J.; Vukmirovic, M. B.; Xu, Y.; Mavrikakis, M.; Adzic, R. R. *Angew. Chem., Int. Ed.* **2005**, *44*, 2132–2135.
(14) Wakisaka, M.; Suzuki, H.; Mitsui, S.; Uchida, H.; Watanabe, M. *J. Phys. Chem. C* **2008**, *112*, 2750–2755.
(15) Kaukonen, M. *J. Phys. Chem. B* **2007**, *111*, 12543–12550.
(16) Blomberg, M. R. A.; Siegbahn, P. E. M. *J. Comput. Chem*. **2006**, *27*, 1373–1384.
(17) Siegbahn, P. E. M.; Blomberg, M. R. A. *Biochim. Biophys. Acta* **2007**, *1767*, 1143–1156.
(18) Siegbahn, P. E. M.; Blomberg, M. R. A. *J. Phys. Chem. A* **2008**, *112*, 12772–12780.

Table 1. Free-Energy Levels of the CcO Model Proposed by Kaukonen[15] and Blomberg and Siegbahn[16] [a]

	at CcO potential and pH = 7		at U = 0 V and pH = 0	
	G^{15} (eV)	G^{16}	G^{15} (eV)	G^{16} (eV)
R + 4(H^+ + e^-)	2.06	2.00	4.92	4.92
P_M + 4(H^+ + e^-)	1.98	1.78	4.84	4.70
F + 3(H^+ + e^-)	1.19	1.28	3.32	3.48
O + 2(H^+ + e^-)	0.85	0.59	2.28	2.05
E + (H^+ + e^-)	0.51	0.13	1.24	0.86
R + 2H_2O (l)	0	0	0	0

[a] Energy levels are shown under physiological and standard conditions. The intermediates correspond to the intermediates of the overall reaction mechanism illustrated in Figure 2a.

these new studies are not included in this paper because they do not report a full catalytic cycle. This could change the values for the O and E levels slightly. The calculated values are collected in Table 1. There have also been calculations for the MCOs,[19] but they are presently not as detailed because the rereduction process of the active site is still to be elucidated.

CcO is the final enzyme in the respiratory chain, situated in the mitochondrial membrane, where it converts molecular oxygen in the gas phase into water. Coupled to the free-energy release is a transmembrane proton transfer, which creates a charge gradient across the membrane, subsequently utilized in the production of adenosine triphosphate. For this to occur, eight protons are taken from the inside of the membrane, four of which are released to the outside of the membrane, while the rest are consumed in the formation of water.[3,20] The overall reaction is

$$O_2(g) + 8H^+(in) + 4e^- \rightarrow 2H_2O + 4H^+(out) \quad (5)$$

Electrons are donated by cytochrome *c*, a small electron shuttling protein with a redox potential of ~0.3 V vs SHE. With the potential of 0.815 V, for dioxygen reduction at pH = 7, this results in a free-energy gain of ~2 eV for a complete catalytic cycle, without considering the membrane potential. In order to facilitate this complicated strategy, CcO employs a total of four redox centers, where Cu_A and heme a are only involved in electron transfer while Cu_B and heme a_3 form the binuclear center (BNC), where the reduction of dioxygen occurs.[3] Over the years, much attention has been devoted especially to the redox centers of the BNC. Various spectroscopic experiments, along with X-ray crystallography, have played a pivotal role in elucidating the structure of intermediates in the catalytic cycle. It has been established that Cu_B is a redox-active complex, where Cu alternates between the 1+ and 2+ oxidation states, while heme a_3 has a porphyrin ring with a redox-active Fe alternating between the 2+, 3+, and 4+ oxidation states.[21−26] By combination of the intermediate structures with experimentally determined parameters, a general reaction mechanism has now been accepted, where dioxygen binds to the fully reduced transition metals of the BNC, which subsequently delivers three electrons to the dioxygen, with the fourth electron being delivered by a nearby tyrosine residue. This is followed by rereduction of the BNC and the tyrosine residue, supposedly by four subsequent (H^+ + e^-) steps, where the electrons are delivered via Cu_A and heme a. Eventually, two water molecules are released and the BNC returns to the fully reduced state. The overall mechanism is illustrated in Figure 2a, while the structure of the BNC is illustrated in Figure 2b.

Figure 2a shows that, despite the fact that the enzyme reaction is quite different from the inorganic counterpart, the enzymatic process also proceeds via a series of (H^+ + e^-) transfer steps. We can therefore compare the energy levels of the intermediates found in the enzymes with those described in the mechanism for Pt(111).

The free energies found in refs 15 and 16 (in Table 1; G^{15} and G^{16}, respectively) need to be converted into standard free-energy values (pH = 0, potentials relative to SHE). The overall change in the free energy of the full catalytic cycle at physiological conditions is ~2.0 eV. At standard conditions, the chemical potential of (H^+ + e^-) is so that the overall change in the free energy of the ORR is 4.92 eV. That means that in the conversion to standard conditions the chemical potential of each (H^+ + e^-) changes with (4.92 eV − 2.06 eV)/4 for column 3 and (4.92 eV − 2.00 eV)/4 for column 4 in Table 1. Each free-energy state is changed according to the number of (H^+ + e^-). In the first reaction step, R to P_M, dioxygen is bound and reduced at the BNC. This process can be viewed simply as a local rearrangement with no charge-transfer steps occurring, and it is seen in Table 1 that the energy gain obtained under standard conditions compared to physiological conditions is unaltered for this step. Figure 3 shows the energy levels of the CcO intermediates calculated from Kaukonen and from Blomberg and Siegbahn at different potentials. We note that the simulations of the enzyme are done with a different kind of basis set and a different functional for describing the nonclassical part of the electron−electron interaction than what was used for the Pt surface. However, because only differences between binding energies are considered, we expect that the comparison is robust concerning the calculation setup.

(19) Vayner, E.; Schweiger, H.; Anderson, A. B. *J. Electroanal. Chem.* **2007**, *607*, 90–110.
(20) Wikström, M. *Nature* **1977**, *266*, 271–273.
(21) Van Gelder, B. F.; Beinert, H. *Biochim. Biophys. Acta* **1969**, *189*, 1–24.
(22) Kitagawa, T.; Ogura, T. *Prog. Inorg. Chem.* **1997**, *45*, 431–479.
(23) Yamaguchi, H.; Tomizaki, T.; Tsukihara, T. *Science* **1998**, *280*, 1723–1729.
(24) Ishimura, S.; Yoshikawa, S. *Proc. Natl. Acad. Sci. U.S.A.* **2003**, *100*, 15304–15309.
(25) Oda, K.; Ogura, T.; Appelman, E. H.; Yoshikawa, S. *FEBS Lett.* **2004**, *570*, 161–165.
(26) Yoshikawa, S.; Muramoto, K.; Shinzawa-Itoh, K.; Aoyama, H.; Tsukihara, T.; Ogura, T.; Shimokata, K.; Katayama, Y.; Shimada, H. *Biochim. Biophys. Acta* **2006**, *1757*, 395–400.

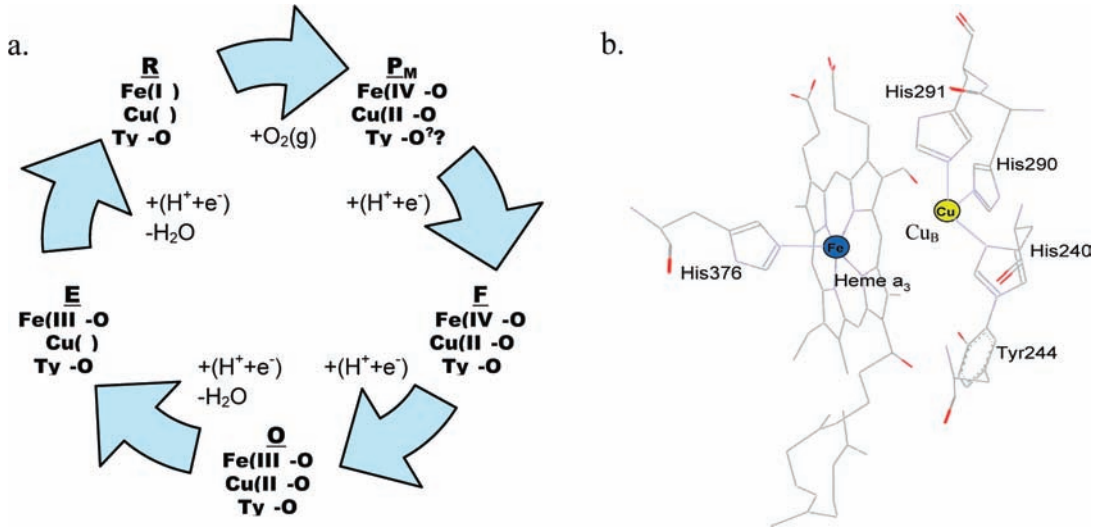

Figure 2. (a) Generally accepted overall reaction mechanism of CcO. Modified from ref 14. Underlined letters refer to the various intermediates in the mechanism, with the states of the redox centers shown below. The R to P_M step includes binding and full reduction of dioxygen in a local rearrangement reaction. In P_M to R, the oxidized redox centers are rereduced by four subsequent ($H^+ + e^-$) charge-transfer steps, which result in the release of two water molecules and regeneration of the active site. (b) Schematic of the active site, in bovine CcO (1V55), which facilitates the binding and reduction of dioxygen with subsequent release of water molecules. Histidine ligands directly coordinated to the Fe-containing heme a_3 and the Cu-containing Cu_B centers are shown along with Tyr244, which delivers the fourth electron to dioxygen.

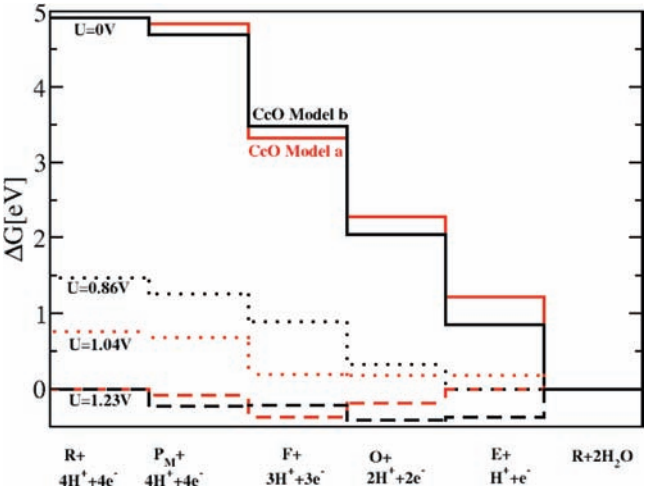

Figure 3. Free-energy diagram for oxygen reduction of two CcO models: model a;[15] model b.[16] In addition to 0 and 1.23 V, energy levels are shown at the potential where the least exothermic ($H^+ + e^-$) charge-transfer step reaches equilibrium, corresponding to the theoretical overpotentials.

Small variations in the free energies are observed between the two enzyme calculations because they use slightly different models for the enzyme. In Blomberg and Siegbahn's model, the theoretical overpotential of 1.23 V − 0.86 V = 0.37 V is seen to originate from the last ($H^+ + e^-$) transfer step where E is converted to R, while the overpotential in Kaukonen's model, 1.23 V − 1.04 V = 0.19 V, originates from two isoenergetic steps, F to O and O to E. Considering the energies at the potential $U = 1.23$ V, it is observed that all intermediates in both models are bound too strongly to the active site. Another interesting observation at $U = 1.23$ V is the similar level of the most stable intermediates in each model. The most stable intermediate in Blomberg and Siegbahn's model is the O intermediate at −0.41 eV, while the most stable intermediate in Kaukonen's model is the F intermediate at −0.36 eV. This similarity is interesting considering the difference in theoretical overpotentials, and it serves to illustrate the importance of having more than one ($H^+ + e^-$) transfer step to overcome the free energy of a too stable intermediate.

Polarization Curves

To allow for a comparison of the turnover rates, or current densities, between the inorganic catalysts and the enzyme models, we will now develop a simple model for the turnover rates. We write the rate constant of each ($H^+ + e^-$) step as

$$k = k_0 \exp[(\Delta G_0 + eU)/k_B T] \quad (6)$$

where k_0 is a prefactor and ΔG_0 is the free-energy change at zero potential. The overall rate is given by the rate of the slowest step at a given potential. This method is a theoretical construct that can be used to compare different catalysts under the assumption that all reaction barriers for proton transfer, in addition to those given by the thermodynamics, are constant. The comparison is on a per site basis so differences in the densities of the active sites are not taken into account in this analysis. In the present case, this means that the model can be used to evaluate the relative ranking of the active sites in the hypothetical situation where they all have the same density at a surface where proton transfer is from an adjacent water layer. The model has been successfully used to describe the effect of alloying on the catalytic properties of Pt surfaces (see Figure 4).

The model polarization curves for the two enzyme models show these sites to be considerably more effective than Pt(111) on a per site basis. Especially, the model by Kaukonen[15] shows a significant current close to the optimal limit of 1.23 V. Another interesting feature of Figure 4 is the agreement between the predicted and experimental polarization curves, observed in the top half of the diagram for the Pt(111) and $Pt_3Ni(111)$ surfaces. In this region, diffusion has negligible effects on the current density. The observed agreement

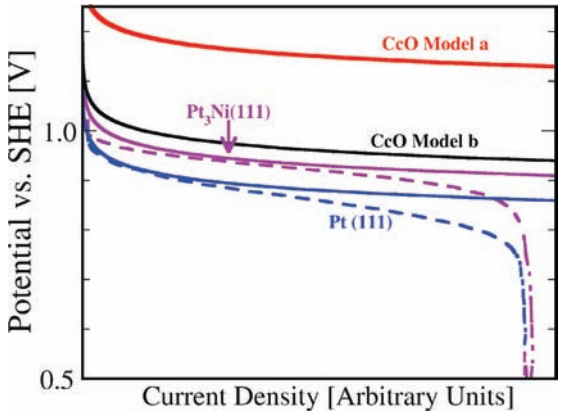

Figure 4. Theoretical and experimental per site polarization curves. The solid lines illustrate theoretical polarization curves of the cathode potential versus current density of the Pt(111), $Pt_3Ni(111)$, and CcO models, as estimated from eq 6: model a;15 model b.16 Here, the least exothermic charge-transfer step is assumed to dictate the overall current density. Equivalent k_0 values are assumed, and no diffusion limits are considered. The dashed lines refer to experimentally determined polarization curves.10 Comparison of the theoretical and experimental curves is only valid at low current densities because diffusion eventually restricts the experimental densities.

supports the assumption of no potential-independent barriers in the rate-determining proton-transfer step of either Pt catalyst.

Discussion

The method described above provides evidence, in terms of reaction energetics, of how CcOs may be able to outperform inorganic oxygen reduction catalysts on a per site basis. This is supported by the observed low overpotentials of the MCOs. Obviously, the density of the active sites and thereby the current and power densities are much smaller for the enzymes than for a surface. The best bioinspired catalyst FeN_4 incorporated in graphitic sheets[27] shows a current density of 1 order of magnitude smaller than Pt and 2 orders of magnitude smaller than Pt_3Ni.[28] The ideal system would have a site density of a metal surface and the catalytic activity per site of the enzyme. A more qualitative evaluation of the differences and similarities among the inorganic and biological catalysts may therefore be in order. Significant differences are obviously inherent in the environment of the catalytic systems, but these will not be addressed here. Instead, we will try to provide a short overview of some of the more chemically related similarities and differences between the systems.

First, looking at the similarities, the four $(H^+ + e^-)$ transfer steps that eventually complete the catalytic cycles of both systems should be mentioned. This is the feature that allows us to make the comparison of the two systems. Another interesting similarity is the possibility of rapid electron transfer. In the inorganic catalysts, rapid electron transfer is available from electrons at the Fermi level, ensuring that this process is not rate-limiting in the overall cycle. The importance of rapid electron transfer is also evident in the enzymes, where rapid electron transfer prevents the release of toxic oxygen radicals.[29] To emphasize this, rates of intermolecular versus intramolecular electron transfer in the MCOs could be mentioned. In MCOs, electrons are delivered from various substrates to a type 1 Cu ion, which resides approximately 13 Å away from the so-called trinuclear cluster. Electrons are redistributed from the type 1 Cu to the trinuclear cluster, which is a three-Cu-ion cluster that provides the scaffold for dioxygen reduction.[30] It is possible to distinguish between the electron-transfer rates from the substrate to the trinuclear cluster, via the type 1 Cu, and again from the trinuclear cluster to dioxygen. The first rate varies significantly from enzyme to enzyme,[31] whereas the second rate is rapid and almost identical among MCOs.[32] Because the Cu ions of the trinuclear cluster all have to be reduced prior to dioxygen binding,[33] this indicates that MCOs are optimized to prevent the release of oxygen radicals despite their varying substrate specificities.

Turning to the differences between the inorganic and enzymatic oxygen reduction catalysts, we first point to the discrepancy in the applied reaction mechanism. In the inorganic catalysts, dioxygen is reduced by four subsequent $(H^+ + e^-)$ charge-transfer steps. In CcO, dioxygen is reduced by four electrons; all transferred are locally in potential-independent reactions, as depicted in the $R \rightarrow P_M$ step of Figure 2a. Interestingly, a similar strategy is employed by the MCOs. This potential-independent reduction can only be slightly exorgenic if the overpotential of the catalytic cycle is to be kept at a minimum because any large release of free energy will have to be overcome in the following $(H^+ + e^-)$ charge-transfer steps. As seen in Table 1, this requirement is fulfilled in the CcO models.

One of the features that allows the enzymes to employ the described mechanism may be the utilization of multiatomic reaction sites.[34] As mentioned, CcOs utilize two different transition-metal ions with a capacity to release a total of three electrons to dioxygen. A similar feature is seen in the MCOs where the three Cu ions of the trinuclear cluster alternate between the 1+ and 2+ states, providing three electrons for dioxygen reduction. As for the CcOs, the last electron is transferred from a nearby donor, namely, the type 1 Cu ion. These reaction sites deviate from the sites on the 111 catalysts, where the binding and reduction of dioxygen occur on a single-type metal atom.

Another feature that may facilitate the described mechanism is the structural elasticity that resides in the enzymes. It is well-known that enzymes are highly dynamical molecules, where motion in and around the active site often facilitates a given reaction. An example of this is observed in the MCOs, where the Cu−Cu distance between two of the Cu ions in the trinuclear cluster changes from ~5 Å in the fully reduced state[35] to ~3.3 Å in the fully oxidized state.[36]

Furthermore, it is interesting to note how the metal ions are assisted by nearby residues in the reactions of CcOs and

(27) Lefèvre, M.; Proietti, E.; Jaouen, F.; Dodelet, J. *Science* **2009**, *324*, 71–74.
(28) Gasteiger, H. A.; Markovic, N. M. *Science* **2009**, *324*, 48–49.
(29) Proshlyakov, D. A.; Pressler, M. A.; DeMaso, C.; Leykam, J. F.; DeWitt, D. L.; Babcock, G. T. *Science* **2000**, *290*, 1588–1591.
(30) Solomon, E. I.; Sundaram, U. M.; Machonkin, T. E. *Chem. Rev.* **1996**, *96*, 2563–2605.
(31) Xu, F. *Biochemistry* **1996**, *35*, 7608–7614.
(32) Bukh, C.; Lund, M.; Bjerrum, M. J. *J. Inorg. Biochem.* **2006**, *100*, 1547–1557.
(33) Cole, J. L.; Tan, G. O.; Yang, E. K.; Hodgson, K. O.; Solomon, E. I. *J. Am. Chem. Soc.* **1990**, *112*, 2243–2249.
(34) Ma, Y.; Balbuena, P. B. *Chem. Phys. Lett.* **2007**, *440*, 130–133.
(35) Messerschmidt, A.; Luecke, H.; Huber, R. *J. Mol. Biol.* **1993**, *230*, 997–1014.
(36) Lee, S.; George, S. D.; Antholine, W. E.; Hedman, B.; Hodgson, K. O.; Solomon, E. I. *J. Am. Chem. Soc.* **2002**, *124*, 6180–6193.

MCOs. For instance, consider the dioxygen-reduction strategy outlined by Blomberg and Siegbahn. Here, it is proposed that protonation of a lysine residue in the vicinity of the BNC lowers the activation barrier of the O−O bond breaking by ∼0.24 eV to a level more consistent with the experimental value.[16]

The above-mentioned examples illustrate some of the features that may be required to employ a reaction mechanism similar to that of the enzymes. The large flexibility of the enzymatic active site stands in sharp contrast to the rigid structure of the inorganic catalysts. This may serve as a guideline to the design of future catalysts.

Conclusion

In this paper, we have shown how oxygen reduction enzymes can be compared directly to inorganic catalysts by applying the previously developed free-energy method. The energy levels of intermediates at pH = 7 for two CcO models were converted to corresponding energy levels at pH = 0. This allowed for a direct comparison with the energy levels in inorganic catalysts. By allowing the cell voltage to drop, we determined theoretical overpotentials and found these to be significantly lower for the enzymes compared to the Pt(111) catalyst. One enzymatic model showed a theoretical overpotential as low as 0.19 V, close to the experimentally determined overpotential of the most efficient oxygen reduction enzyme known: the multicopper oxidase laccase. Finally, we presented a simple rate expression that allowed us to construct theoretical per site polarization curves for each of the catalysts.

Acknowledgment. CAMD is funded by the Lundbeck Foundation. This work was supported by the Danish Center for Scientific Computing.